Data-driven Diversity Antenna Selection for MIMO Communication using Machine Learning

ChienHsiang Wu, ChinFeng Lai*
Department of Engineering Science, National Cheng Kung University, Taiwan
chienhsiang.wu@gmail.com, cinfon@ieee.org

Abstract

With the popularity of wireless application environments, smart antenna technology has completely changed the communication system. In order to improve the quality of wireless transmission, smart antennas have been widely used in wireless devices. Wireless signal modeling and prediction machine learning gradually replaced the traditional smart antenna selection method in the antenna selection solution. This article utilizes mobile devices to adjust the diversity antenna pattern for test verification in a MIMO wireless communication environment. The proposed method manipulates signal parameters through error vector magnitude (EVM) and adds data-driven training data. The results show that the SVM and NN methods proposed in this paper are 10.5% and 14% higher than the traditional EVM calculation methods, respectively. Thereby, realize precise antenna adjustment of mobile devices and improving wireless transmission quality.

Keywords: Antenna selection, Diversity antenna pattern, Data-driven, Error Vector Magnitude

1 Introduction

Till now the wireless transmission has become the mainstream application of communication data. The wireless communication standard is still under development. The clear goals are a higher data rate, lower latency, and more stable transmission performance. The research focuses on improving the quality of wireless transmission in the existing wireless transmission architecture (including hardware, chips, software, and front-end antennas). We believe that improving antenna performance is a direct and cost-effective approach. In traditional antennas, most ways to improve wireless transmission efficiency are to establish compliance with regulations to create the maximum coverage of the antenna radiation pattern. Therefore, the smart antenna [1] design with the variability of the field type should be born. The MIMO systems used parallel transmission of data streams. Multi-channel transmission can significantly improve system throughput, and it has become popular in current and next-generation wireless networks. The antenna selection techniques discussed in the literature improve the transmission efficiency by diversity antenna selection. The antenna selection techniques discussed in this manuscript improve the transmission efficiency by diversity antenna selection. Most literature studies have used ML/DL algorithms to formulate smart antenna adjustment schemes. Most of these methods are based on the premise of experimental design that does not consider space and cost and does simulation test verification. These types of methods may be able to achieve the verification of the theoretical method. Can the actual data be improved in-field wireless transmission?

This article aims to predict the efficiency of the MIMO system [2] by data-driven [3] and related wireless signal data, an adaptive antenna selection technology. The proposed method is to make a complete experimental design in a limited environmental space. It is a design method that uses an external MCU module to drive a variety of antenna options. A complete experimental design is made in a general notebook computer and a MIMO wireless transmission environment in a limited environmental space. In addition to the diversified adaptive antenna architecture, the use of dynamic modeling methods and appropriate algorithms to achieve a better antenna pattern selection and coverage increases the efficiency and stability of the wireless transmission. Its architecture is shown in Figure 1:

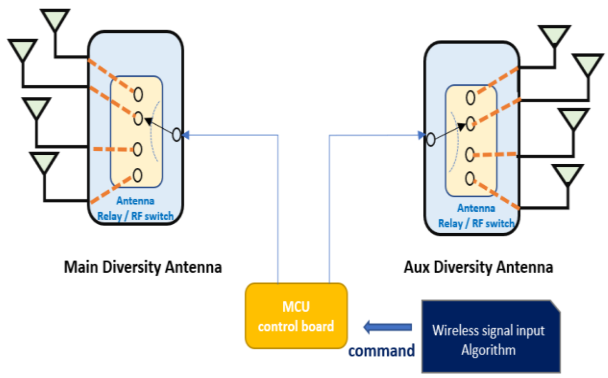

Figure1. Experimental scheme

This article utilizes the multi-class classification algorithm to compare the traditional EVM method, support vector machine (SVM) [4-5], and the neural network (NN) [6-7]. Use the training channel state information (CSI) as the input signal and add data-driven to provide enough channels (data) as training data. Use a variety of classification models to classify and predict the new channel to obtain the best antenna selection. The CSI signal data contains the system's bit error rate (BER), received signal strength indication (RSSI), SNR, EVM, and the data-driven results from different angles in the experiment. This research provides an in-depth understanding of the convergence of machine learning and wireless communication antenna selection.The significant contributions of this paper are: (1) A novel structure expects

*Corresponding Author: ChinFeng Lai; E-mail: cinfon@ieee.org
DOI: 10.53106/160792642022012301001

to fully use existing wireless communication devices to move towards active antennas fully. (2) The CSI and data-driven dynamic modeling of data materials are sufficient to achieve the purpose of timely antenna adjustment. (3) The addition of data-driven data labeling can improve the accuracy of antenna selection and traditional calculation methods by at least 20%. (4) The purpose of this article is to expect such algorithms to be further advanced from the MIMO verification environment to antenna applications such as massive MIMO (mMMIO) [8], Large-scale (LSMIMO) [8-9].

The rest of this article is organized as follows. Section 2 explains some related preparations for this research. In section 3, Methodology of Machine-Learning assisted antenna modeling methods. Section 4, Prediction and validation, Section 5, Conclusion.

2 Related Works

As mentioned in the previous section, this article proposes an application with adjustable antenna patterns in the wireless transmission environment of an existing laptop to enhance better wireless performance at any time. Therefore, we use existing equipment to consider point-to-point MIMO communication as the subject of the experiment, in addition to the CSI-related channel signal information taken, to be closer to the actual transmission application. This article adds the data-driven method to achieve a higher accuracy of antenna selection in the chamber simulation experiment of the labeling.

2.1 Experimental framework

First, this research uses 2 Tx and 2 Rx MIMO antenna transmissions, and the hardware architecture is shown in Figure 1. The structure of this experiment uses main and aux main antenna streams to control four different planar inverted-F antennas (PIFA) [10]. Under this framework, the MCU controls the two-stream antenna to create $C_1^4 \text{x} C_1^4 = 16$ different antenna patterns. Through the adjustment of different antenna patterns, 16 different CSI signal data will be generated. This experiment obtained various x-y, y-z, x-z plane radiation patterns. This experiment obtained various x-y, y-z, z-x plane radiation patterns. Figure 2 and Figure 3 indicate wireless channel 149 as the Main and Aux antenna, x-y plane radiation patterns in the experiment as example patterns.

This article uses Figure 1 as the experimental equipment to obtain wireless signal data at different angles and attenuations in the chamber. Many CSI signal input data, including data-driven, received signal strength indicator (RSSI), signal strength, signal-to-noise ratio (SNR), and BER are used as the basis for antenna adjustment.

2.2 Experimental environment

Under the MIMO transmission architecture, it takes M transmitting and N receiving antennas as an example. The multiple data streams can be spatially multiplexed on M transmitting antennas and received by N receiver antennas. Because multiple data streams are transmitted on the same available frequency band, spatial multiplexing increases the link's capacity. Therefore, the reliability of the link improves in the MIMO environment. Figure 3 below shows the transmission mode of the MIMO antenna, and Figure 4 below represents the CSI [14] signal architecture operating under the MIMO system.

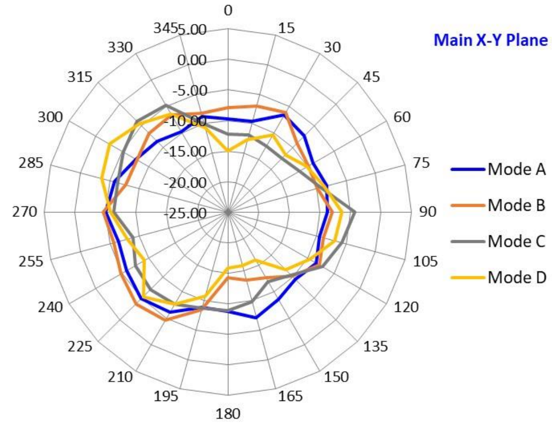

Figure 2. Channel 149, 5745MHz 2D Main x-y plane radiation pattern

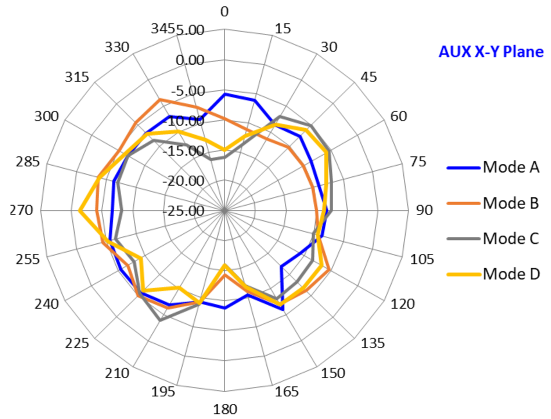

Figure 3. Channel 149, 5745MHz 2D Aux x-y plane radiation pattern

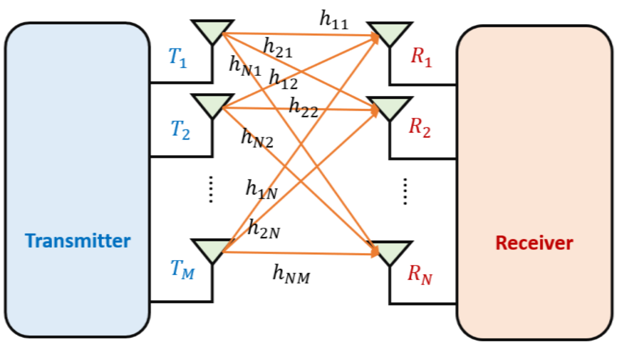

Figure 4. MIMO system representation

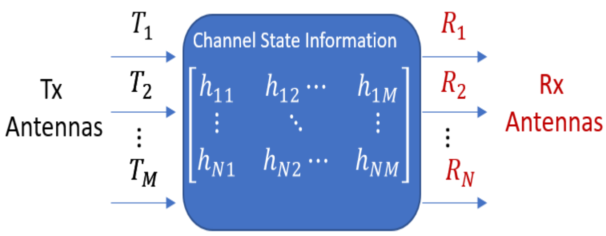

Figure 5. MIMO from a channel perspective

It is represented by Figure 5 above, where h_{ik} represents the channel from the k^{th} transmitting antenna to the i^{th} receiving antenna. Assuming the multipath channel length is l, the signal y_i received by the i^{th} antenna can be expressed as (without noise consideration).

$$y_i = \sum_{k=1}^{N} X_k \times h_{ik} \quad \textbf{(1)}$$

The signal received by the i^{th} antenna is the sum of the channels transmitted by each antenna to i. (This can also be said to be, each receiver antenna not only receives the direct signal intended for it but also receives the signal from other propagation paths) Consider the noise, such as Figure 5 MIMO from a channel perspective. The receiving vector y is represented by the channel transmission matrix H, the input vector x, and the noise vector n as:

$$y = Hx + n \quad \textbf{(2)}$$

In the MIMO environment, the dimension of the channel matrix is NxM. Then equation (2) will be rewritten into a multi-dimensional equation.

Note that the response of the MIMO link is expressed as a set of linear equations.

For the 2x2 MIMO architecture configuration proposed in this article, the received signal vector is expressed as

$$\begin{bmatrix} y_1 \\ y_2 \end{bmatrix} = \begin{bmatrix} h_{11} & h_{12} \\ h_{22} & h_{22} \end{bmatrix} \begin{bmatrix} x_1 \\ x_2 \end{bmatrix} + \begin{bmatrix} n_1 \\ n_2 \end{bmatrix} \quad \textbf{(3)}$$

Following this model, we consider a simple point-to-point communication using the transmitter (Tx) and receiver (Rx) antennas of h_t and h_r as training data in the MIMO 2x2 antenna environment. Select a set of antenna index vectors, $s_n \in R^{n_s \mathrm{x} 1}$, is defined as N = $\{n_1, \ldots, n_S\}$, where the elements of the $s_n$represent the index of the selected antenna [11],

$$y' = \max_{n_s \in N}(H\mathrm{x} + n) \quad \textbf{(4)}$$

Because of the y' in equation (6), the corresponding transmission and reception optimize the actual channel gain. In addition, adding data-driven test results provides the best antenna selection basis for wireless signal judgment.

Finally, the transmission matrix (also called CSI) determines the applicability of the MIMO technology and affects the wireless transmission capacity. The CIS is constant in the single input single out (SISO) wireless channel and does not change bit by bit. Therefore, knowledge of CSI in the SISO link is usually not required because steady-state SNR characterizes it. In the case of a fast-fading channel, the channel state information changes rapidly. The channel change can be decomposed into spatially separated sub-channels by using the MIMO feature. Under this characteristic, to obtain the CSI (at the transmitter or receiver), develop a system design that incorporates this information into the smart antenna. It can achieve rapid adjustment and stably improve the wireless transmission quality, which is the purpose of this article.

2.3 Data preparation

As mentioned previous section, this article is based on the experimental equipment of the traditional laptop plus the signal data obtained in the chamber and related instruments. Among them, the chamber is shown in Figure 6 and Figure 7.

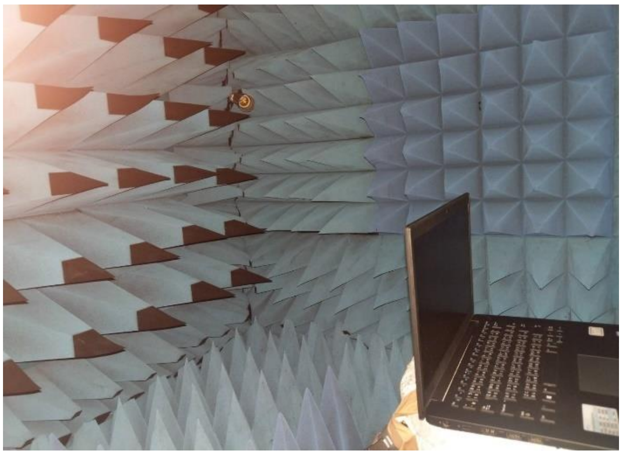

Figure 6. Laptop for testing in a chamber

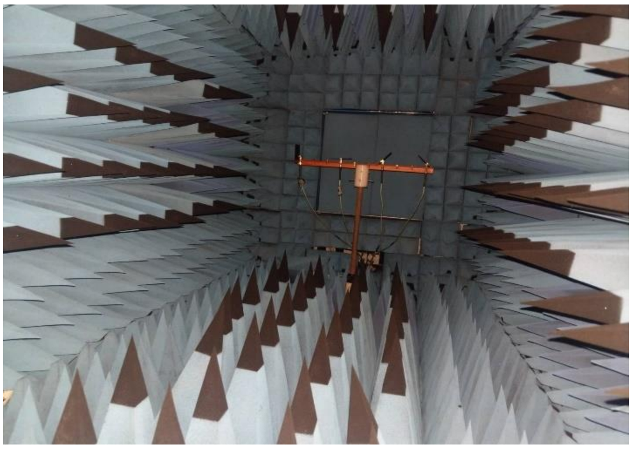

Figure 7. 2x2 MiMO test environment in a chamber

Different signal attenuation and adjustable horizontal angles in this environment are added because the chamber isolation factor will have less noise interference CSI signal data. This experiment uses the attenuator from 0 dB to 50 dB from the horizontal angle of 0 degrees to 360 degrees. For example, Table 1 shows the level of 0 degrees, and the attenuation is 0 dB plus the calculated EVM value [12-13].

However, during the experiment, it was found that signal fluctuation sometimes occurs, especially when the signal condition is weak or at high dB attenuation. The reasons for signal fluctuation are as follows. The received signal strength is the magnitude of the vector sum of various propagation paths. The strength of the received signal is a random variable, and the propagation environment is time-varying, so the fading of the wireless channel is also time-varying. To reduce the signal fluctuation of the wireless, the accuracy of antenna selection deteriorates. To reduce this phenomenon, the method used in this article is to use the EVM calculation method to pre-process the data. EVM is generally used to evaluate the modulation quality of the transmitter signal, avoiding the use of multiple parameters to characterize the transmitted radio frequency signal. It is a valuable indicator of the entire signal quality during the development and design process. Figure 8 illustrates the schematic diagram of the EVM. Its practice and equation (5) are as follows: The method used in this article is to use the EVM calculation method to pre-process the data. The result is shown in Table 1 in the red number column. Table 1 shows the red number column.

Table 1. CSI signal data with horizontal degree 0 and attenuation 0 dB

Att.	Ant	Angle	Data-Driven	CCK	OFDM			1 Stream			2 Stream antenna 1			2 Stream antenna 1		
dB	mode	horizontal plane	bits/sec	rssi	rssi	evm	snr	rssi	evm	snr	rssi	evm	snr	rssi	evm	snr
0	0	0	671.712	0	75	32	31	0	0	0	70	27	30	67	29	31
0	1	0	646.344	0	75	32	31	0	0	0	70	27	30	70	29	29
0	2	0	673.199	0	74	33	31	0	0	0	71	28	30	64	30	31
0	3	0	669.614	0	75	32	31	0	0	0	70	28	30	68	29	30
0	4	0	669.863	0	75	32	31	0	0	0	71	27	30	67	29	31
0	5	0	646.674	0	75	32	31	0	0	0	71	26	30	70	28	29
0	6	0	675.411	0	75	33	31	0	0	0	71	28	30	63	30	31
0	7	0	660.308	0	75	32	31	0	0	0	71	28	30	68	29	30
0	8	0	659.205	0	76	32	31	0	0	0	71	27	30	67	29	31
0	9	0	659.882	0	76	32	31	0	0	0	71	28	30	70	29	29
0	10	0	666.122	0	76	33	31	0	0	0	71	28	30	64	29	31
0	11	0	670.945	0	76	32	31	0	0	0	71	29	30	68	29	30
0	12	0	661.179	0	76	32	31	0	0	0	72	27	30	67	29	31
0	13	0	663.736	0	76	32	31	0	0	0	72	27	30	70	29	29
0	14	0	666.945	0	76	33	31	0	0	0	72	28	30	64	29	31
0	15	0	669.992	0	76	32	31	0	0	0	72	28	30	68	29	30

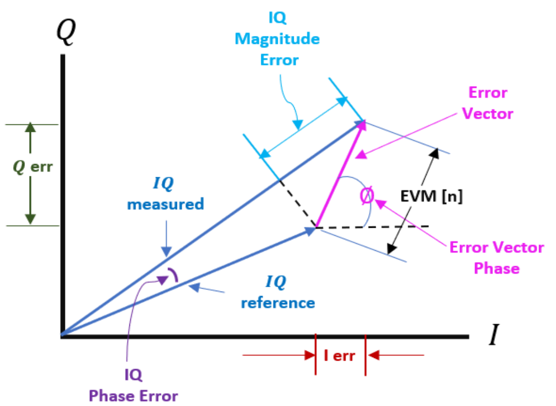

Figure 8. Schematic diagram of error vector signal definition

The n is symbol index, Ierr is I Ref – I Meas, Qerr is Q Ref – Q Meas, and the A is a normalization factor.

$$EVM[n] = \frac{\sqrt{\mathrm{Ierr}[n]^2 + \mathrm{Qerr}[n]^2}}{\mathrm{A}} \tag{5}$$

3 Methodology

In generating the training set, the training sample is the input of the learning system, which is called the input variable, feature, predictor variable, or attribute. From Figure 5, the channel matrix H_m (or vector) of M $h_r \times h_t$ is used for training in the transmission in communication. Because the training sample is a real-valued vector, it is necessary to process channels for N real-valued features. For example, the angle, signal value (real part), and attenuation (imaginary part) are substituted by h_{ij}, where h_{ij} is the (i, j)th complex number-the value element of H_m. There is a manipulated real-valued matrix $T \in R^{MxN}$ and the corresponding class label vector c = $[c_1, \ldots, c_M]^T$ in this mode. It uses the labeled training data set, namely T and c. To build a learning system: a trained multi-class classifier whose input is CSI and output is the index of the selected antenna set (mode). In addition, the training samples must be normalized, that is, feature normalization, to avoid apparent deviations in training. For example, the procedures used in this study are as follows:

3.1 SVM

The SVM algorithm was designed originally for binary classification problems. When dealing with multi-classification problems, it is necessary to construct a suitable multi-class classifier that can generally be divided into two categories:

(1) Direct method: modifies directly on the target function. Merge the parameter solution of multiple classification planes into one optimization issue and realize multi-class classification by solving the optimization problem 'one trial'. This method seems simple, but its computational complexity is high and challenging to implement. It is only suitable for minor issues.

(2) Indirect method: The construction of multiple classifiers is mainly realized by combining multiple two classifiers. Common methods are "one-versus-one" and "one-versus-all".

The method chosen in this experiment is the "one-versus-all" binary classification method in the indirect method. The detailed procedure is as follows.

Algorithm 1. SVM

This article utilizes Figure 8 to Figure 11 to illustrate the flow of the SVM algorithm.

Input: From the CSI signal value, which includes different angles, the signal value obtained in the attenuation includes RSSI, SNR, EVM, and data-driven results.

Output: Antenna mode result $\{a_1, . . . , a_s\}$.

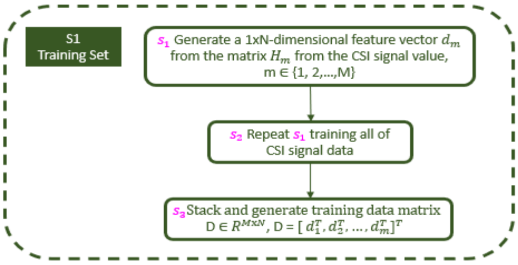

Figure 9. SVM initial procedure

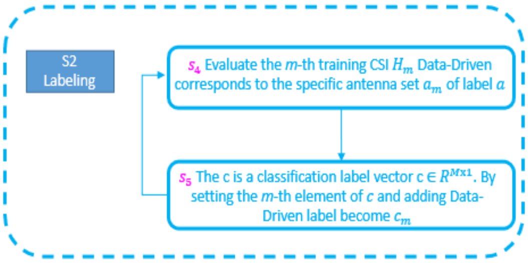

Figure 10. SVM Labeling procedure

In s_4, for multi-class SVM, the method of this experiment is to set $A \subseteq \{a_1, a_2, \dots, a_N\}$ with different attenuations, and N is the number of attenuations. Then repeat $s_4$and s_5 for all m CSI samples H_m.

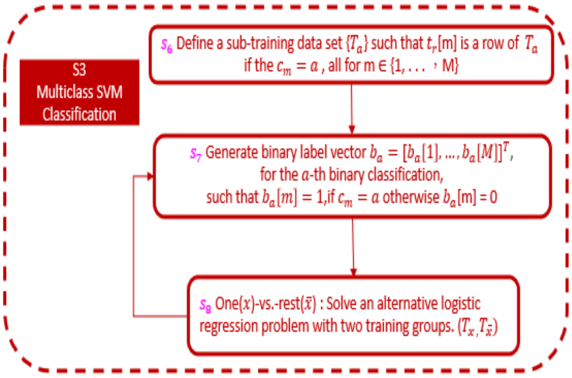

Figure 11. The SVM classification procedure

We use |*A*| binary classifiers. Each classifier recognizes one category from other categories, that is, the one-versus-all binary classification method. Such as procedure S3. Define $\{T_a\}$ for all $a \in A$. Then, we perform an SVM to classify the two training groups T_{a_i} and T_{a_j}, where T_{a_i}, T_{a_j} are two different attenuation label matrices. T vector from T_{a_i} by eliminating rows.

Generate a binary label vector, $z_a = [z_a[1], \dots, z_a[M]]^T$ For the a^{th} binary classification, if $z_a[m] = 1$ if $c_m = a$, otherwise z_a[m] = 0. After the step s_7, we constructed a matrix {TNM} to represent the feature set:

$$\mathrm{T} = \begin{bmatrix} z_{11} & \cdots & z_{1M} \\ \vdots & \ddots & \vdots \\ z_{N1} & \cdots & z_{NM} \end{bmatrix} \quad \textbf{(6)}$$

Suppose there are n types of samples to be classified. In this experiment, n=16, then n classification functions will need to be constructed. For example, the i^{th} SVM separates the samples of the i^{th} class from all other classes. For this reason, the category number of the sample should be revised again. The i^{th} sample category is marked as +1, and the labels of other categories are marked as -1. The class with the largest classification function output is selected as a prediction in the classification process.

For M training samples, it belongs to the k^{th} category, $(x_1,y_1),\dots\dots,(x_M,y_k)$, $x_1 \in R^m$, is an m dimensional feature vector and $y_i \in \{$ 1,2,..., M$\}$, i=1,2,…, M. The i-th SVM solves the following series of problems.

$$\min_{A^i \varepsilon^j} \frac{1}{2} (w^i)^T w^i + \mathrm{C}\sum_{j=1}^{M} \xi_j \quad \textbf{(7)}$$

$$\text{Class of x} \triangleq \arg \max_{i=1,\dots,M} (w^i)^T \ \Phi(\mathrm{x}) + b^i \quad \textbf{(8)}$$

The training sample x_i is mapped to a high-dimensional space through Φ. C is the penalty function used to balance the bias, and overfitting will reduce the number of misclassified samples. The penalty function as:

$$c_k(z) = (-1)^k z + 1 \quad \textbf{(9)}$$

When classification, assign the category of the unknown sample to the category with the largest value of the classification function:

Repeat S_8. for all $a \in \{1, . . . , |A|\}$.

3.2 ANN

ANN [15] has strong parallel distributed processing capabilities. In addition to solid robustness and fault tolerance to noise nerves, it can also fully handle complex nonlinear relationships. Therefore, this experiment uses the characteristics of ANN to solve the problem of multi-antenna selection. Thereby appropriate signal fields can be quickly and accurately selected to achieve the application of smart antennas. The method uses the signal value changes in M Tx antennas and N Rx antennas to predict the best signal antenna. Especially in the power minimization problem, the optimal solution exists. The proposed NN uses a supervised learning method to update network parameters, using mean square error (MSE) as a metric in the loss function. The choice of backpropagation ANN in this experiment is mainly due to its versatility, fast convergence rate, and other advantages. Take x1, x2... and other CSI antenna signal data as input and pass through a four-layer network with the first layer, two as the hidden layer, and one output layer. It comprises 600 sets of neurons and is defined by the rule function, and the third layer consists of a set of neurons with linear functions. Its structure is shown in Figure 12.

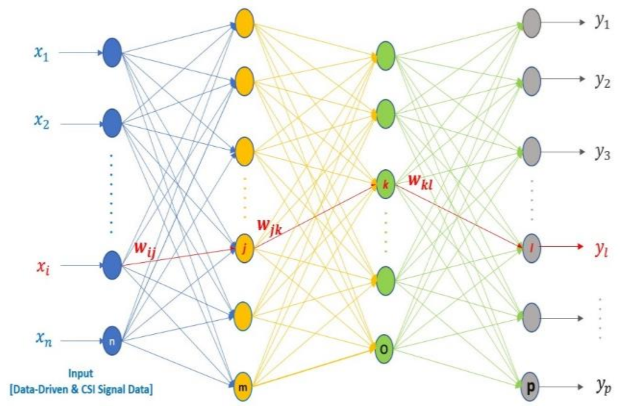

Figure 12. NN structure

The Figure 12 above, the NN architecture of this experiment i, j, k, is the input layer, j, k is the hidden layer, and l is the neuron of the output layer. First, calculate the net weight input.

$$X = \sum_{i=1}^{n} x_i w_i - \theta \quad \textbf{(10)}$$

The n is the number of inputs (CSI signal + data-driven value), θ is the neuron threshold. Here we use sigmoid as the activation function. The main reason is to ensure that the output of the neuron is between 0 and 1. The error (signal) of the z^{th} iteration of neuron l can be defined as :

$$e_l(z) = y_{dl}(z) - y_l(z) \quad \textbf{(11)}$$

$y_{dl}(z)$ is the expected output of the z^{th} iteration of neuron l.

$y_l(z)$ is the expected output of the z^{th} iteration of neuron l.

Weight modification:

$$w_{kl}(z+1) = w_{kl}(z) + \Delta w_{kl}(z) \quad \textbf{(12)}$$

$\Delta w_{kl}(z)$ weight correction

The weight correction of the multilayer network in this experiment is:

$$\Delta w_{kl}(z) = \alpha \ x \ y_k(z) \ \text{x} \ \delta_l(z) \quad \textbf{(13)}$$

$\delta_l(z)$, It is the error gradient of the neuron at the z^{th} iteration of the output layer and α is the learning rate here. The error gradient is :

$$\delta_l(z) = \frac{\partial y_l(z)}{\partial X_l(z)} \ x \ e_l(z) \quad \textbf{(14)}$$

$X_l(z)$ input for the net weight of the z^{th} iteration neuron l.
The sigmoid function:

$$\delta_l(z) = \frac{\partial\left\{\frac{1}{1+e^{-X_l(z)}}\right\}}{\partial X_l(z)} \ \text{x} \ e_l(z) = \frac{e^{-X_l(z)}}{\{1+e^{-X_l(z)}\}^2} \ \text{x} \ e_l(z) \quad \textbf{(15)}$$

$$\delta_l(z) = y_l(z) \ x \ (1 - y_l(z)) \ x \ e_l(z) \quad \textbf{(16)}$$

the $y_l(z) = \frac{1}{1+e^{-X_l(z)}}$

For the weight correction of the hidden layer, take the input layer as an example to do the calculation:

$$\Delta w_{ij}(z) = \alpha \ x \ x_i(z) \ \text{x} \ \delta_j(z) \quad \textbf{(17)}$$

Where $\delta_j(z)$ is the error gradient of the hidden layer neuron j

$$\delta_j(z) = y_j(z) \ \text{x} \ (1 - y_l(z)) \ \text{x} \ \sum_{k=1}^{o} \delta_k(z) w_{jk}(z) \quad \textbf{(18)}$$

the $y_j(z) = \frac{1}{1+e^{-x_j(z)}}$

$$x_j(z) = \sum_{i=1}^{n} x_i(z) w_{ij}(z) - \theta_j \quad \textbf{(19)}$$

In this way, the hidden layer's weight correction and gradient error are calculated, and the backpropagation neural network can be derived.

Algorithm 2. ANN

This article utilizes Figure 13 to Figure 15 to illustrate the flow of the ANN algorithm.
Input: From the CSI signal value, which contains the signal value obtained from different angles and attenuation, including data such as RSSI, SNR, EVM, and data-driven results.
Output: Antenna mode, $y \in \{y_1, y_2, \ldots, y_n\}$.

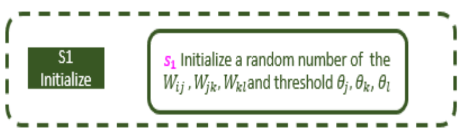

Figure 13. ANN initial procedure

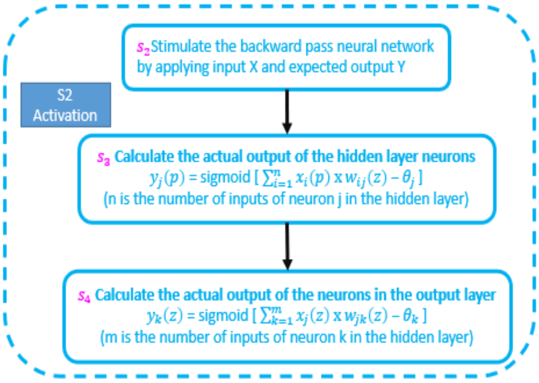

Figure 14. ANN activation functions procedure

Stimulate the backpropagation ANN by applying the input $x_i(z)$ and the expected output $y_{dl}(z)$, where z is the number of iterations.

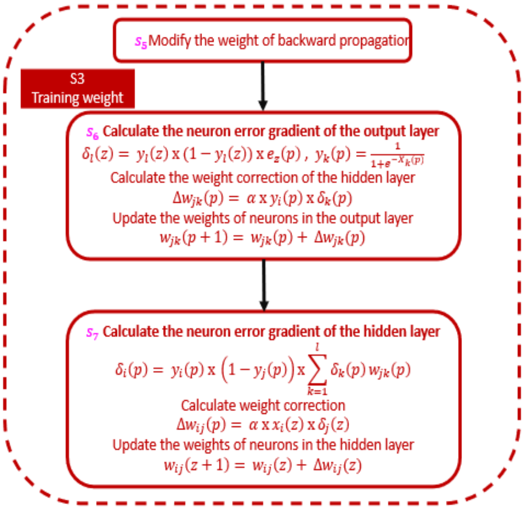

Figure 15. ANN training weight procedure

After S3 is modified, the weight of the ANN is passed to it.

The number of iterations p+1 go back to step 2 and repeat the above process until the deviation requirement is satisfied.

This section details description of these three algorithm methods EVM, Multi-class SVM, and backpropagation NN, applied to the calculation process of this experiment. The following section will describe the results of these three algorithms on the diversity antenna selection mechanism comprehensively compare the accuracy of antenna selection.

4 Prediction and Validation

This experiment is based on the chamber at wireless channel 149, frequency 5745MHz, to obtain the signal data. It includes different horizontal angles, adjusted the dB value of different attenuators, and the data-driven emphasized in this experiment. Under such an experimental environment, the beamforming and interference generated by MIMO have been reflected in the test's real data-driven value. Estimate based on measurement data to verify the performance. This experiment obtained more than 5000 sets of training data selected from the collected measurement data.

4.1 Multi-class SVM prediction

When using the One-Versus-All SVM algorithm [16] to classify faces, select the radial basis function (RBF), adjust the penalty factor and the kernel parameters. In this experiment, the SVM classification function is 16. This experiment adjusts the penalty factor C and the radial kernel parameter σ. A good classifier will obtain from training for data-driven and antenna mode selection. The measurement data is obtained in the darkroom and uses multi-class SVM to classify one-versus-all and cross-validation methods. This experiment uses traditional EVM to calculate the test data obtained from various horizontal angles and signal strengths. This EVM data is used as the result of traditional smart antenna selection and imported into the entire data set and used as the SVM and NN in the experiment as input data for training. Cross-validation with complete data is shown in Figure 16 and Figure 17. From the comparison of experimental results, the best accuracy of Multi-class SVM and the EVM measurement method is improved by 10.5%.

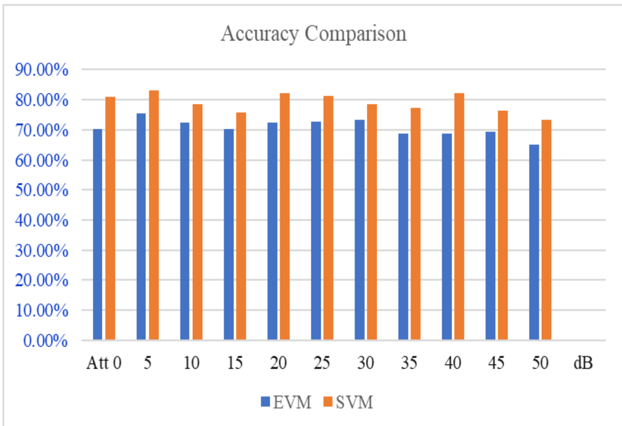

Figure 16. Comparison of accuracy between EVM and SVM

4.2 Backpropagation NN prediction

From the various signal parameters of Table 1, including 15 input neurons including data-driven, there are 16 neurons in the output layer, with two hidden layers. In Figure 16, the error is plotted for the 6,000 epochs. Note how the error is saturated at the value 4.15e-13, which is very close to 0.0

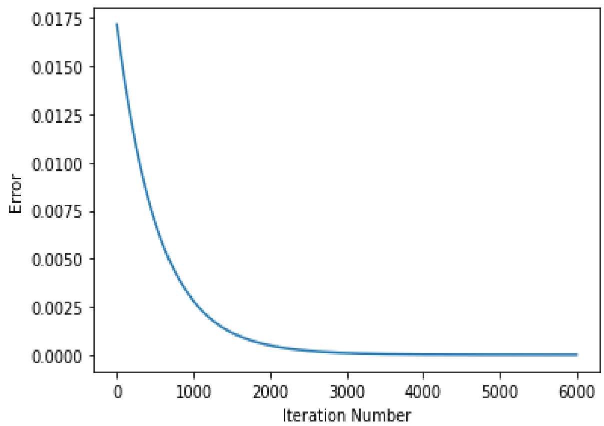

Figure 17. The chart of iteration number and error

The next figure shows how the predicted output changed by iteration. The output is saturated at the value 0.8458, very close to 0.845.

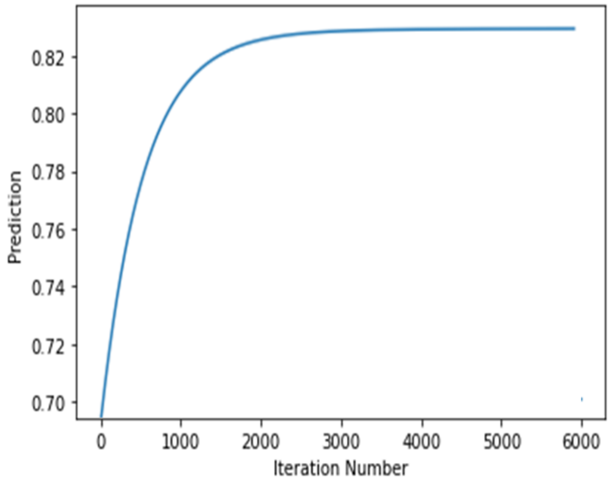

Figure 18. The chart of iteration number and prediction

The verification is shown in Figure 19. Compared with the experimental results, the best accuracy rate of backpropagation NN [17] and the multi-class EVM measurement method are improved by 14%.

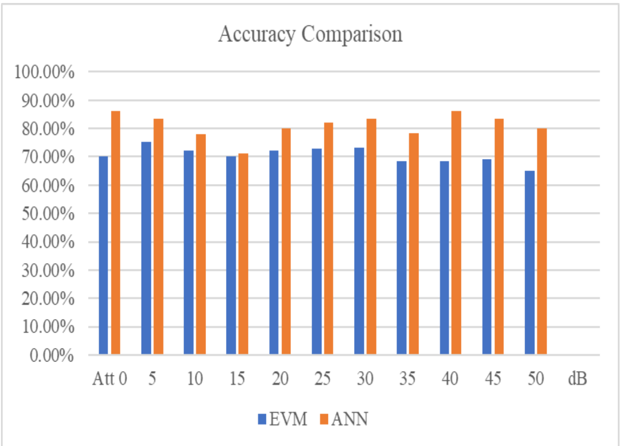

Figure 19. Comparison of accuracy between EVM and ANN

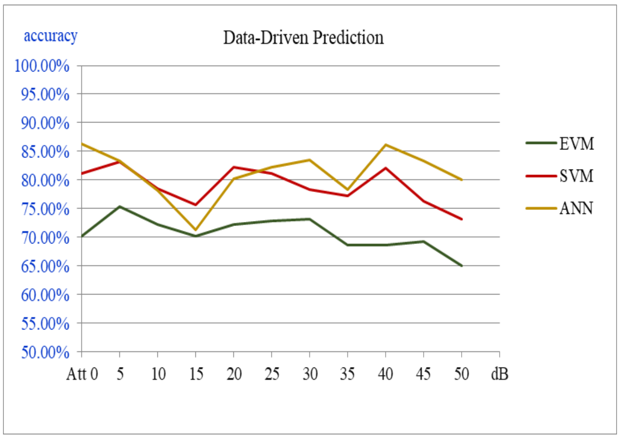

Figure 20. Comparison with the EVM, SVM, and ANN antenna selection prediction

Table 2. Antenna selection accuracy prediction

Antenna Selection Prediction			
Attenuation (dB)	EVM	SVM	NN
0	0.702	0.811	0.863
5	0.754	0.832	0.833
10	0.723	0.785	0.781
15	0.702	0.757	0.713
20	0.723	0.822	0.802
25	0.728	0.812	0.822
30	0.732	0.784	0.845
35	0.676	0.712	0.783
40	0.686	0.821	0.862
45	0.693	0.763	0.833
50	0.651	0.732	0.801
average	0.707	0.790	0.812

From Table 2 above, it can be observed that the average accuracy of the multi-call SVM and traditional EVM algorithms used in this experiment is higher than 8.3%. However, the average of the individual attenuation values at 40dB is higher than 14%. The average accuracy of the backpropagation NN and traditional EVM algorithms used is higher than 10.5%. The average attenuation value at 40dB also has an 18% accuracy improvement.

This result presents two manners. First, the EVM algorithm used in this experiment significantly improves against wireless signal fluctuation, especially in a weak signal environment. Second, multi-class machine learning with the multi-class SVM and backpropagation NN can effectively improve antenna selection accuracy because the method in this experiment is data-driven, which will also enhance the quality of wireless transmission.

5 Conclusion

The method proposed in this paper uses machine learning such as SVM and ANN for diversity antenna selection in a MIMO environment. The simulation results using data-driven in the chamber show that the prediction results of these two machine methods are more effective than the traditional EVM prediction model. It is enough to illustrate the results of using machine learning methods and adding data-driven antenna selection schemes in a simulation in the chamber. The results of this experiment are used in general wireless transmission applications with specific practical value.

Acknowledgements

This study is conducted under the “New generation transport deep learning intelligent system Project” of the Institute for Information Industry which is subsidized by the Ministry of Economic Affairs of the Republic of China.

References

[1] A. Singh, J. Kyllonen, S. Caduc, J. Shamblin, M. Garg, A. Horie, Compact smart antenna system for improving probability of detection, *2017 IEEE International Symposium on Antennas and Propagation &*

USNC/URSI National Radio Science Meeting, San Diego, CA, USA, 2017, pp. 1383-1384.

[2] H. S. Hussein, S. Hussein, E. M. Mohamed, Efficient channel estimation techniques for MIMO systems with 1-bit ADC, *China Communications*, Vol. 17, No. 5, pp. 50-64, May, 2020.

[3] Y. Lv, R. Chi, Data-driven adaptive iterative learning predictive control, *2017 6th Data Driven Control and Learning Systems (DDCLS)*, Chongqing, China, 2017, pp. 374-377.

[4] S. Bhandari, H. P. Zhao, H. Kim, P. Khan, S. Ullah, Packet scheduling using SVM models in wireless communication networks, *Journal of Internet Technology*, Vol. 20, No. 5, pp. 1505-1512, September, 2019.

[5] B. R. Taub, SVM based method for multi-equalizer optimization, *2019 IEEE International Conference on Microwaves, Antennas, Communications and Electronic Systems (COMCAS)*, Tel-Aviv, Israel, 2019, pp. 1-4.

[6] Z. Ghorrati, A New Adaptive Learning algorithm to train Feed-Forward Multi-layer Neural Networks, Applied on Function Approximation Problem, 2020 *Fourth IEEE International Conference on Robotic Computing (IRC)*, Taichung, Taiwan, 2020, pp. 501-505.

[7] H. Luo, Q. Hou, Y. Liu, L. Zhang, Y. Li, Fuzzy Clustering Algorithm for Interval Data Based on Feedback RBF Neural Network, *Journal of Internet Technology*, Vol. 21, No. 3, pp. 799-810, May, 2020.

[8] S. Zhong, Z. Zheng, A Joint Iterative Quantization and Channel Estimation Scheme for One-Bit Massive MIMO Systems, *Journal of Internet Technology*, Vol. 21, No. 1, pp. 51-59, January, 2020.

[9] M. B. Salman, G. M. Güvensen, T. Ciloglu, Investigation of Effects of PA Non-linearities on the Fully Digital Massive MIMO Systems, *2020 28th Signal Processing and Communications Applications Conference (SIU)*, Gaziantep, Turkey, 2020, pp. 1-4.

[10] S. P. Biswal, S. Das, A dual band MIMO PIFA for WLAN application, *2017 USNC-URSI Radio Science Meeting (Joint with AP-S Symposium)*, San Diego, CA, USA, 2017, pp. 121-122.

[11] S. Kim, Transmit Antenna Selection for Precoding-Aided Spatial Modulation, *IEEE Access*, Vol. 8, pp. 40723-40731, February, 2020.

[12] J. V. Hof, C. D. Martino, S. Malotaux, M. Squillante, M. Marchetti, L. Galatro, M. Spirito, Vector gain based EVM estimation at mm-wave frequencies, *2020 95th ARFTG Microwave Measurement Conference (ARFTG)*, Los Angeles, CA, USA, 2020, pp. 1-5.

[13] Z. Zeng, M. Shao, Impact of EVM on Network Performance, *2018 International Conference on Sensor Networks and Signal Processing (SNSP)*, Xi'an, China, 2018, pp. 13-16.

[14] C.-H. Hsieh, J.-Y. Chen, C.-M. Kuo, P. Wang, End-to-End Deep Learning-Based Human Activity Recognition Using Channel State Information, *Journal of Internet Technology*, Vol. 22, No. 2, pp. 271-281, March, 2021.

[15] Z. D. Zaharis, T. V. Yioultsis, C. Skeberis, T. D. Xenos, P. I. Lazaridis, G. Mastorakis, C. X. Mavromoustakis, Implementation of antenna array beamforming by using a novel neural network structure, *2016 International Conference on Telecommunications and Multimedia (TEMU), Heraklion, Greece, 2016, pp. 1-5.*

[16] L. Zhang, X. Huang, Multiple SVM-RFE for multi-class gene selection on DNA Microarray data, *2015 International Joint Conference on Neural Networks (IJCNN)*, Killarney, Ireland, 2015, pp. 1-6.

[17] C. Tarver, L. Jiang, A. Sefidi, J. R. Cavallaro, Neural Network DPD via Backpropagation through a Neural Network Model of the PA, *2019 53rd Asilomar Conference on Signals, Systems, and Computers*, Pacific Grove, CA, USA, 2019, pp. 358-362.

Biographies

ChienHsiang Wu is studying for a Ph.D. in Engineering Science, National Cheng Kung University, Taiwan. He specializes in embedded systems, networking data security, cloud edge computing, and active antenna research.

ChinFeng Lai is a professor at Department of Engineering Science, National Cheng Kung University and Department of Computer Science and Information Engineering, National Chung Cheng University since 2016. He received the Ph.D. degree in Department of Engineering Science from National Cheng Kung University, Taiwan, in 2008. He received Best Paper Award from IEEE 17th CCSE, 2014 International Conference on Cloud Computing, IEEE 10th EUC, IEEE 12th CIT . He has more than 100 paper publications and 9 papers selected to TOP 1% most cited articles by Essential Science Indicators (ESI). He is an associate editor-in-chief for Journal of Internet Technology and serves as editor or associate editor for IET Networks, International Journal of Internet Protocol Technology, KSII Transactions on Internet, Information Systems and Journal of Internet Technology. His research focuses on Internet of Things, Big Data Analysis and Edge Computing etc. He is an IEEE Senior Member since 2014.